

Offset phase locking of noisy diode lasers aided by frequency division

E. N. Ivanov,^{1,a)} F.-X. Esnault,^{2,b)} and E. A. Donley²

¹University of Western Australia, School of Physics M013, 35 Stirling Highway, Crawley 6009 WA, Australia

²National Institute of Standards and Technology, 325 Broadway, Boulder, Colorado 80305, USA

(Received 16 May 2011; accepted 3 August 2011; published online 31 August 2011)

For heterodyne phase locking, frequency division of the beat note between two oscillators can improve the reliability of the phase lock and the quality of the phase synchronization. Frequency division can also reduce the size, weight, power, and cost of the instrument by excluding the microwave synthesizer from the control loop when the heterodyne offset frequency is large (5 to 10 GHz). We have experimentally tested the use of a frequency divider in an optical phase-lock loop and compared the achieved level of residual phase fluctuations between two diode lasers with that achieved without the use of a frequency divider. The two methods achieve comparable phase stability provided that sufficient loop gain is maintained after frequency division to preserve the required bandwidth. We have also numerically analyzed the noise properties and internal dynamics of phase-locked loops subjected to a high level of phase fluctuations, and our modeling confirms the expected benefits of having an in-loop frequency divider. © 2011 American Institute of Physics. [doi:10.1063/1.3627535]

I. INTRODUCTION

Phase-coherent lasers are used in many important scientific and industrial applications including, for example, laser beam combining,¹ atom interferometry,² quantum optics^{3,4} and recently, chip-scale optical atomic clocks.⁵ Since the first attempts at laser phase synchronization,⁶ technological advances in laser frequency stabilization in the late 1990s have enabled optical phase control with residual errors in the microradian range.⁷ Achieving such a level of phase stability is still a serious challenge, but many practical applications of phase-locked lasers require a more modest degree of phase control, on the order of tens of milliradians. This level of noise performance has been consistently demonstrated with extended cavity diode lasers (ECDLs),^{8,9} but phase-locking of solitary diode laser chips with much higher levels of intrinsic phase fluctuations than ECDLs demands a more significant effort owing to the much higher demands on the bandwidth of the control electronics. At the same time, it is desirable to use solitary diode lasers for applications because of their compactness and relative simplicity.

In this work, we discuss phase-locking high phase noise lasers with large heterodyne frequency offsets with an emphasis on the effects of having an in-loop frequency divider. In Sec. II, we present two experimental phase lock loop configurations, one of which utilizes a frequency divider. We also present the effect of the frequency division on the phase noise of the optical beat note and discuss the limitations of the technique. In Sec. III, we discuss a numerical time-domain approach to noise analysis of a phase-locked loop (PLL) focused on optimal choice of the loop filter, and we model the carrier collapse phenomenon^{10,11} in a PLL containing frequency dividers. Finally, in Sec. IV, we analyze the dynamics of different types of PLLs under the influence of high-intensity phase fluctuations.

II. PLL EXPERIMENTS

Figure 1(a) shows a conventional laser phase synchronization system used for achieving large heterodyne frequency offsets. It features a microwave frequency synthesizer which sets a “coarse” separation between the two lasers and down-converts the optical beat note to the RF frequency range where its phase can be compared to that of a reference RF source. The resulting error voltage from the output of a digital phase detector steers the frequency of a “slave” laser such that the mean frequency difference between two lasers is $f_{\mu w} \pm f_{RF}$, where $f_{\mu w}$ and f_{RF} are the microwave and the RF frequencies, respectively. In general, the phase detector can be an analog mixer, but it is also convenient to use a digital phase/frequency detector (DPFD). DPFDs have a larger capture range but also reduce the PLL bandwidth due to internal delays.

An alternative configuration for an optical PLL is shown in Fig. 1(b). It takes advantage of an in-loop frequency divider, which reduces the size, weight, power, and cost of the PLL due to the elimination of the microwave synthesizer. It also permits higher accuracy of phase stabilization due to the lower intrinsic phase fluctuations exhibited by frequency dividers, as compared to microwave synthesizers (discussed below). We have used both systems in Fig. 1 to phase-lock a distributed feedback (DFB) laser to a frequency-stabilized distributed Bragg reflector (DBR) laser locked to the D1 line of ⁸⁷Rb.¹²

The linewidth of a typical DFB/DBR diode laser is of the order of 1 MHz, which results in the beat note spectrum between two lasers shown in Fig. 2. To identify the type of phase fluctuations responsible for laser line broadening, we measured the power spectral density of phase fluctuations of the optical beat note as a function of the Fourier frequency F with a microwave delay-line frequency discriminator (FD) consisting of a power divider with two arms of unequal length terminated at a double-balanced mixer (DBM). The voltage at the output of the DBM is a periodic function of signal

^{a)}Electronic mail: eugene@physics.uwa.edu.au.

^{b)}Also at SYRTE, Observatoire de Paris, 61 avenue de l’Observatoire, 75014 Paris, France.

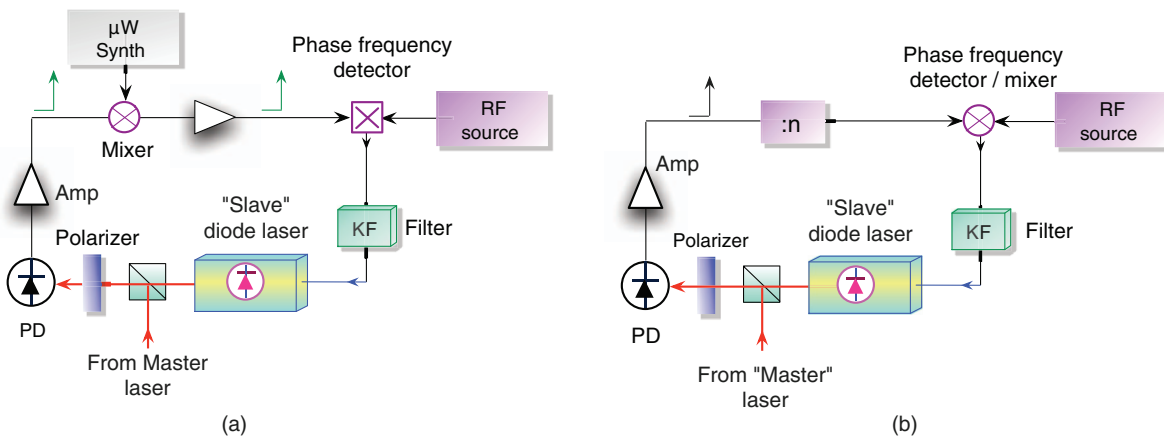


FIG. 1. (Color online) Schematic diagrams of heterodyne phase-locking configurations. (a) A typical diode laser phase synchronization system. (b) A simplified phase synchronization configuration that takes advantage of an in-loop frequency divider and eliminates the microwave synthesizer.

frequency f given by $u = \chi\sqrt{P_{\text{RF}}}\cos(2\pi f\tau_D)$, where χ is the DBM power-to-voltage conversion efficiency, P_{RF} is the power at the RF port of the DBM, and τ_D is the differential propagation delay between the two arms.

To enable the phase noise measurements, τ_D is adjusted to set the mixer dc voltage close to zero. This maximizes the frequency-to-voltage conversion efficiency du/df and its linear dynamic range Δf_{FD} . Also, it makes the frequency discriminator insensitive to power fluctuations of the input signal. We measured $du/df = 14$ mV/MHz and $\Delta f_{\text{FD}} = 50$ MHz. The latter parameter was sufficiently large to permit linear conversion of laser phase/frequency fluctuations into voltage noise.

The spectral density of the phase fluctuations of the optical beat note, S_{ϕ}^{opt} , was measured at 6.8 GHz, which corresponds to the ground state hyperfine splitting in ^{87}Rb . From 100 Hz to 10 MHz, S_{ϕ}^{opt} fits closely to a simple power law: $S_{\phi}^{\text{opt}} = (8 \times 10^{13}/F^4 + 1 \times 10^6/F^2)$ rad²/Hz. The first term corresponds to random walk of the laser frequency, while the

second term is due to random walk of the laser phase.¹³ This type of phase noise spectrum is typical for most free-running oscillators regardless of their physical makeup and operation frequency. The highly diverging $1/F^4$ term is usually related to the temperature fluctuations.

Curve 2 in Fig. 2 shows a spectrum of a frequency divided ($n = 32$) optical beat note. It looks almost “monochromatic” compared to the spectrum of the beat note extracted directly from the photodiode (curve 1). This is because of a factor of 32^2 reduction in the power of phase fluctuations. Frequency division simplifies the process of phase acquisition and reduces the likelihood of cycle slips.¹⁴ The power of the frequency-divided optical beat note in Fig. 2 is higher than that of original signal. This is due to the use of an active divider with a built-in power amplifier.

Next, we measured intrinsic phase fluctuations of a number of commercial frequency dividers. This was accomplished by splitting the power of a microwave signal (at 6.8 GHz) between two frequency dividers ($n = 16$), whose output signals (425 MHz) were recombined in quadrature at an RF mixer. When referred to 6.8 GHz, the phase noise spectrum of an individual frequency divider fit the power law $10^{-6}/F^2$ rad²/Hz, which is >10 dB lower than the phase noise of a typical microwave synthesizer operating at the same frequency.

Spectra of optical beat notes between two phase-synchronized diode lasers are shown in Fig. 3. Here, curves 1 and 2 correspond to the PLLs shown in Figs. 1(a) and 1(b), respectively. The error signals for both data sets were generated with DPFs. In both cases, the fraction of the total power confined to the central carrier was between 70% and 75%. The loop filter for each PLL contained two parallel arms: a broadband gain stage and an integrator. The gain stage was capable of introducing a phase lead of $\sim 50^\circ$ for the Fourier frequencies from 100 kHz to 7 MHz. The integrator was needed to suppress the random walk fluctuations of laser phase difference. The effect of the integrator on the beat note spectra is visible in Fig. 3 as a ~ 5 dB deep well in the immediate vicinity of the carrier. The DPDF of the first PLL (Fig. 1(a)) was a relatively slow device performing the phase comparison at ~ 80 MHz, while the DPDF of the frequency-divided PLL (Fig. 1(b)) operated

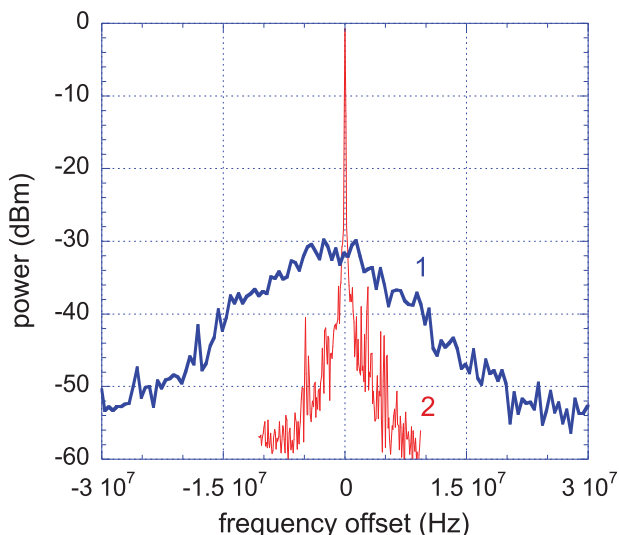


FIG. 2. (Color online) Spectra of optical beat notes at 6.8 GHz (1) and at 212 MHz (2). The PLL is off.

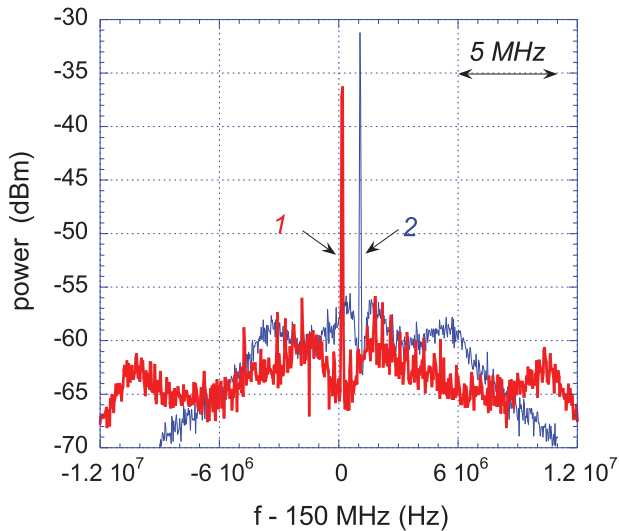


FIG. 3. (Color online) Spectra of optical beat notes of two phase-locked lasers. PLL with microwave synthesizer (1); PLL with frequency divider (2) ($n = 8$).

at 850 MHz. In both cases, the phase-lock was very reliable, with the lasers staying locked for days without human intervention.

While studying the frequency-divider-based PLL (Fig. 1(b)), we also exchanged the 850 MHz DPFDF with a double-balanced mixer. The idea was to increase the PLL bandwidth, since the mixer has a much faster response than the DPFDF. What was lost in this swap was the frequency discrimination provided by the DPFDF, which resulted in significantly reduced reliability of the phase-lock with only a marginal increase of the loop bandwidth, prompting us to go back to using the DPFDF.

The weak effect on the PLL bandwidth associated with the introduction of a mixer instead of a DPFDF could be explained by the relatively large time delay around the control loop, most of which was due to the light propagation through free space from the slave laser to the photodiode. Our simulations show that reducing the time delay is more important for extending the PLL bandwidth than broadening the laser frequency response. Assuming our current diode laser (with the crossover frequency of ~ 1 MHz), a PLL bandwidth close to ~ 43 MHz could be achieved for a time delay of 0.5 ns, provided one can tolerate the servo overshoot of 6 dB at a Fourier frequency of ~ 124 MHz. Therefore, miniaturization of the PLL physical package is a key future step for improving the coherence of phase-locked noise diode lasers.¹⁵

We also measured the power spectral density of residual phase fluctuations between two lasers, S_{ϕ}^{res} . The spectrum was inferred from that of the voltage fluctuations at the output of the digital phase detector (the PLL in Fig. 1(a) was used), knowing its phase-to-voltage conversion efficiency (~ 0.5 V/rad). Within the PLL bandwidth, S_{ϕ}^{res} was almost independent of the Fourier frequency and equal to $\sim 3 \times 10^{-9}$ rad²/Hz. The noise power $P_{\phi}^{res} = \int S_{\phi}^{res}(f)df$ computed over the frequency range of 10 MHz was slightly less than 0.4 rad². This is consistent with our measured fractional power of $\sim 70\%$ confined to the carrier of the optical beat note.¹²

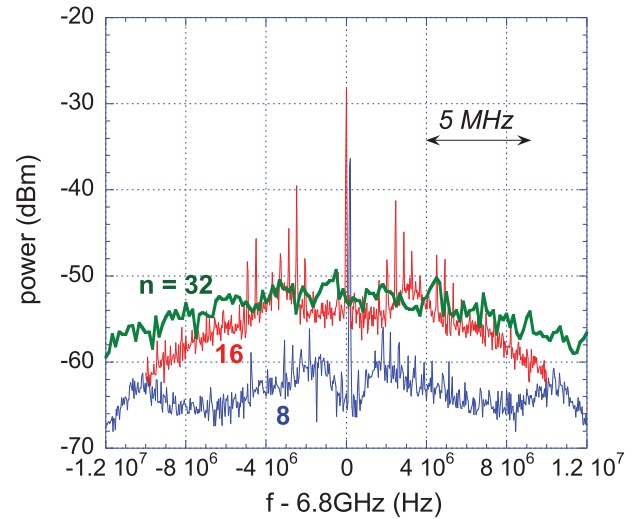


FIG. 4. (Color online) Spectra of optical beat notes with the PLL enabled for various frequency division ratios. Resolution bandwidth = 30 kHz.

It should be noted that our first attempts to phase-lock two diode lasers using a frequency divider were unsuccessful. The problem was related to the use of high frequency division ratios n . This is illustrated by the data in Fig. 4, which shows the spectra of optical beat notes at $n = 8, 16$, and 32 . As n increases from 8 to 16, the PLL bandwidth decreases from roughly 7 MHz to 2 MHz. At $n = 32$, the carrier of the beat note is no longer visible above the noise background. This loss of PLL bandwidth followed by the carrier collapse is due to two factors. First, the introduction of a frequency divider reduces loop gain by a factor of n . To maintain the same quality of phase synchronization one has to increase gain of the loop filter. This increase, however, is accompanied by a phase lag at the high Fourier frequencies due to the limited gain-bandwidth product of the operational amplifiers used in the loop filter, which reduces the loop phase margin and limits the maximum practical division factor.

Secondly, it is a simplification to characterize a frequency divider by its division ratio n . Such an approximation is only valid at the relatively low Fourier frequencies F . At Fourier frequencies above a few MHz, the frequency division ratio behaves as a complex function of F . The use of large division ratios lowers the Fourier frequency at which the complex nature of the frequency divider's transfer function becomes significant.

Figure 5 illustrates the transformation of a beat note spectrum by the frequency divider. Here, one spectrum corresponds to the output of a photodiode, while another – to the output of a frequency divider ($n = 8$). As expected, the fraction of the power confined to the carrier of the frequency divided beat note is much higher than that of the photodiode's signal. Within the experimental accuracy, these fractions are 0.99 and 0.7, respectively. Interestingly, even at $n = 32$ when the optical beat note has no carrier, the frequency divided signal features a narrow central peak ~ 20 dB above the noise pedestal.

The above experiments indicate that frequency dividers can simplify PLL structure and reduce cost without imposing

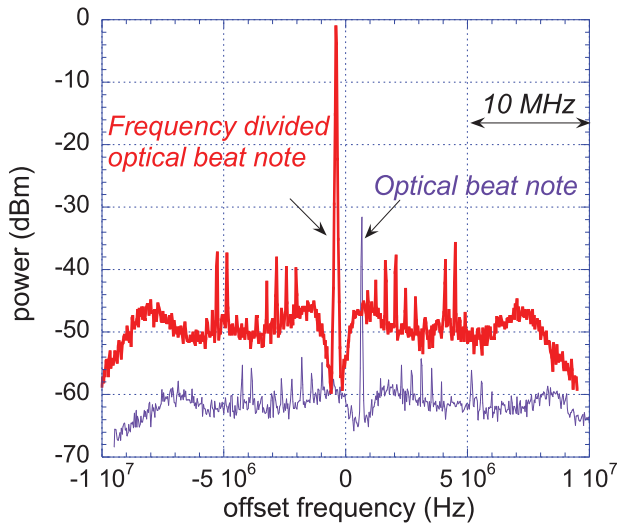


FIG. 5. (Color online) Spectra of optical beat notes at 6.8 GHz and 850 MHz. The PLL is on. Resolution bandwidth = 30 kHz.

any restrictions on the PLL bandwidth at moderate indexes of frequency division ($n = 8$). On the other hand, as pointed out in Refs. 8 and 16 the presence of a frequency divider does not eliminate the need for broadband noise suppression.

III. NUMERICAL PLL NOISE ANALYSIS

To mimic the phase fluctuations in real oscillators, we used a set of numerical Monte Carlo algorithms that make use of a random-number generator to simulate white phase noise with a Gaussian probability distribution. Then we integrated the resulting noise to produce a random walk of phase $\phi(t)$ with power spectral density inversely proportional to the square of the Fourier frequency $S_\phi(F) = \alpha/F^2$, where α is a constant characterizing the noise intensity. To test our algorithms, we computed the Fourier spectra of RF signals that have a random walk of phase $u = A \cos(\omega_0 t + \phi(t))$ and confirmed that they have the Lorentzian shape with the linewidth $\Delta\nu$ consistent with the Schawlow-Townes formula: $\Delta\nu \simeq \pi\alpha$.

In real oscillators, the power spectral density of close-to-carrier phase fluctuations is inversely proportional to the third or the fourth power of Fourier frequency. To generate the latter noise type (random walk of frequency), we integrated the white noise from our Monte Carlo algorithms twice. Having computed spectra of the RF signals with a random walk of frequency, we confirmed that their shapes were best described by a Gaussian profile.

To model phase fluctuations of a real oscillator we used a mixture of uncorrelated random walks of frequency and phase with different weighting coefficients. The resulting power spectrum of the simulated phase fluctuations is shown in Fig. 6 (trace 1). When simulating random phase variations, we used $N = 2^{21}$ equidistant samples spread over an observation period interval $T_{obs} = 0.8$ s. This corresponded to a sampling period of $\Delta t = 0.4 \mu\text{s}$, which was sufficient to analyze signals with frequencies up to $f_{max} \leq 1/(2\Delta t) \simeq 1$ MHz while avoiding aliasing and prohibitively long computation

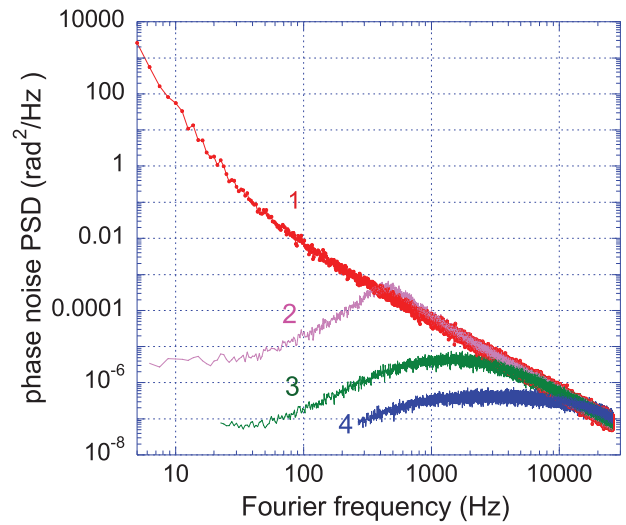


FIG. 6. (Color online) Effect of PLL on phase noise spectra: PLL is disabled (1); “narrow-band” PLL is on (2); “medium-band” PLL is on (3); and “broad-band” PLL is on (4). A power law fit to the “free-running” spectrum gives $S_\phi(F) \simeq 3 \times 10^5/F^4 + 100/F^2$ rad²/Hz. The filtered spectra are truncated at low frequency, since it was not possible to correctly reproduce them without increasing T_{obs} and N .

periods.^{13,17} Both N and T_{obs} strongly affect the shape of the RF spectrum. An increase in N broadens the RF spectrum, while an increase in T_{obs} narrows it. For the simulations in this section, we kept N and T_{obs} fixed while varying parameters of the PLL.

PLL filtering of the phase fluctuations was modeled in the time domain with the filtered phase noise $\Phi(t)$ computed as a convolution of free-running phase fluctuations $\phi(t)$ and PLL impulse response $g(t)$:

$$\Phi(t) = \int_{-\infty}^t \phi(x)g(t-x)dx. \quad (1)$$

For discrete variables, the convolution integral (Eq. (1)) is replaced with the convolution sum,

$$\Phi_k = \sum_{n=0}^{N-1} \phi_n g_{k-n}, \quad (2)$$

where Φ_k and ϕ_n are the sequences of real numbers corresponding to the sampled phase differences between two oscillators with the PLL enabled and disabled, respectively. Sequence g_k corresponds to the sampled impulse response $g(t)$, which was derived analytically from the inverse Laplace transform of the PLL noise suppression factor $\eta(F)$.

The convoluted process Φ_k is longer than the “input” one ϕ_n . Thus, if sequences ϕ_n and g_k contain a total of N and M samples, respectively, then the overall length of the convoluted noise is $N + M - 1$. For this reason, the process Φ_k needs to be truncated to N samples to avoid transient effects at the end of the observation time interval.

By varying the loop gain and, therefore the loop bandwidth, we computed the spectra of the filtered phase fluctuations shown in Fig. 6. The phase noise spectra given by traces 2, 3, and 4 correspond to the three cases dubbed as “narrow-band,” “medium-band,” and “broad-band” PLLs,

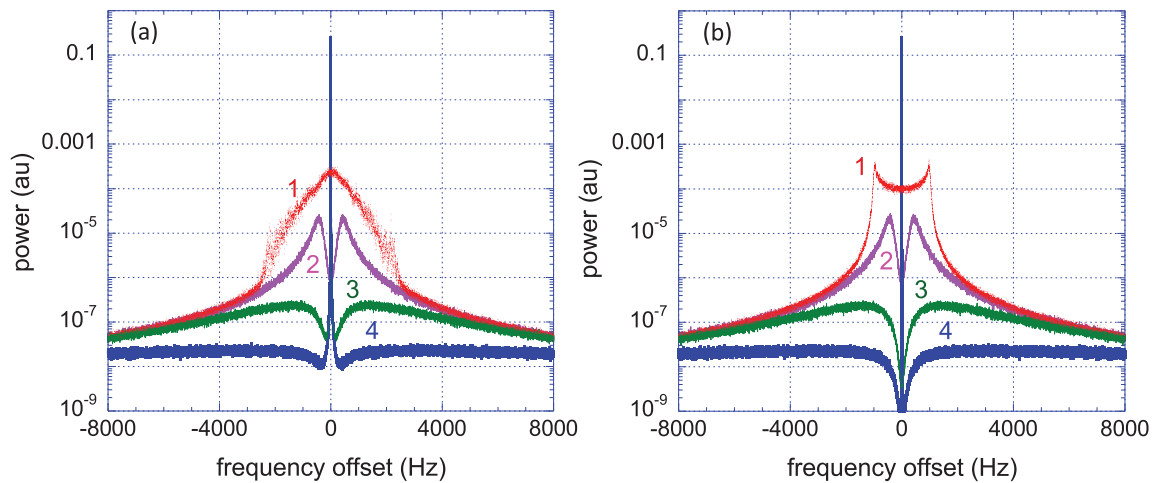


FIG. 7. (Color online) Effect of the PLL on the power spectra of simulated beat notes in the case of a purely random phase modulation (a) and a mixture of random phase noise and low-frequency sinusoidal modulation (b): PLL is disabled (1), “narrow-band” PLL is enabled (2), “medium-band” PLL is enabled (3), and “broad-band” PLL is enabled (4).

respectively, with the loop bandwidth increasing progressively from 300 Hz to 3 kHz and to 10 kHz.

From Fig. 6, it is clear that a PLL with a single integrator limits the power of the filtered phase fluctuations Φ despite the highly divergent nature of the “input” phase noise $\phi(t)$. We calculate the power of the filtered phase fluctuations as 0.22 rad^2 (trace 2), 0.022 rad^2 (trace 3), and 0.008 rad^2 (trace 4).

We also computed spectra of the “RF” signals $u = A \cos(2\pi f_0 t + \phi)$ and $v = A \cos(2\pi f_0 t + \Phi)$ to visualize the effect of the PLL on the beat note spectra between oscillators. The RF spectra $S_u(f - f_0)$ and $S_v(f - f_0)$, where f_0 was assumed to be 100 kHz, are shown in Fig. 7(a). Here, traces 1 through 4 show the RF spectra of the beat notes whose phase noise was computed earlier (curves 1 through 4 in Fig. 6, respectively).

The 3 dB linewidth of the “free-running” beat note (trace 1, Fig. 7(a)) is close to 1.5 kHz. This is five times broader than the bandwidth of the narrow-band PLL, but despite such an unfavorable bandwidth-to-linewidth ratio, the corresponding RF spectrum (trace 2, Fig. 7(a)) features a narrow central spike, which suggests that our estimate for the total power of phase fluctuations ($\delta\phi^2 \simeq 0.22 \text{ rad}^2$) is reasonable.

When comparing spectra 1 and 2 (Fig. 7(a)), one may wonder why the narrow-band PLL narrows the spectrum of the beat note well outside its bandwidth of 300 Hz. Such “strange at first glance” behavior is a result of cancellation of phase fluctuations with $1/F^4$ power spectral density, which dominate the spectrum of a free-running oscillator at frequencies below ~ 50 Hz (see Fig. 6). These spectral components are well within the PLL bandwidth and, therefore, strongly suppressed by it.

To support this explanation we analyzed the effect of the PLL on the RF spectra having sinusoidal phase modulation of large magnitude. We modulated the phase of a free-running oscillator sinusoidally with amplitude of 100 rad and frequency of 10 Hz and included random walk fluctuations ($1/F^2$) with the power spectral density found earlier for the

spectra in Fig. 6. The resulting RF spectrum is shown by trace 1 in Fig. 7(b). The large-scale phase modulation gives rise to a nearly rectangular shape of the RF spectrum with the width of $\sim 2 \times 100 \text{ rad} \times 10 \text{ Hz} = 2 \text{ kHz}$. Enabling the narrow-band PLL (trace 2 in Fig. 7(b)) reduces the amplitude of phase modulation from 100 rad to ~ 0.1 rad, resulting in a spectral shape determined mostly by the $1/F^2$ noise term and virtually identical to that shown by trace 2 in Fig. 7(a).

To explain our carrier-collapse observations for high frequency division factors, we multiplied up the signals from Fig. 7(a) to simulate the use of a frequency divider. Assuming that the RF spectra in Fig. 7(a) represent those at the output of the divider, we computed the corresponding RF spectra at its input. Once again, we computed filtered phase fluctuations $\Phi(t)$ and then power spectra of the frequency-multiplied signals defined as $u = A \cos(n\omega_0 t + n\Phi(t))$. The RF spectra computed for $n = 8$ are shown in Fig. 8. Here, spectra labeled as 1 through 4 originate from those with the same labels in Fig. 7. Frequency multiplication of the beat note corresponding to the narrow-band PLL (trace 2 in Fig. 7) leads to the collapse of the carrier to the noise pedestal.^{10,11} This is a consequence of the high power of phase fluctuations of the frequency-multiplied signal: $n^2\Phi^2 = 64 \times 0.22 \simeq 14 \text{ rad}^2$. Thus, the modeling agrees with our observations in Sec. II, where the indication of phase synchronous operation did not always translate from the down-converted signal to the multiplied beat note. Broadening the PLL bandwidth helps to prevent carrier collapse. In this respect, extending the bandwidth of a single integrator is much more effective than an increase in the number of integrators.

We can formally introduce a signal-to-noise ratio parameter SNR for the RF spectra in Fig. 8, defining it as a ratio of carrier power to the maximum spectral density of noise power. For a broadband PLL characterized by the flat noise pedestal around the carrier: $\text{SNR} \sim 1/n^2$, where n is the frequency multiplication factor. In the case of a narrow-band PLL, the SNR decreases much faster with n leading to an earlier carrier collapse.

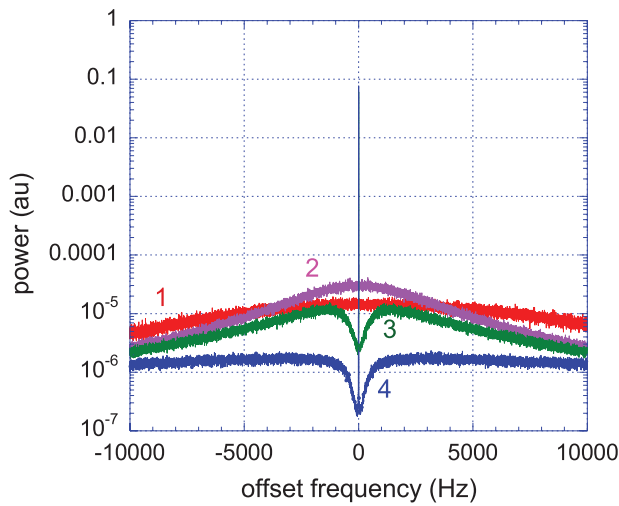


FIG. 8. (Color online) Simulated power spectra of frequency-multiplied beat notes: PLL is disabled (1), “narrow-band” PLL is enabled (2), “medium-band” PLL is enabled (3), and “broad-band” PLL is enabled (4). The carrier frequency was 800 kHz, N was 2^{21} , and the number of averages was 128. Phase locking with a narrow carrier is observed only in the cases 3 and 4.

IV. DYNAMICS OF A PLL SUBJECTED TO HIGH INTENSITY PHASE NOISE

High-intensity frequency fluctuations in solitary diode lasers can easily upset the stationary operation of the PLL, causing cycle slips or total loss of lock. In this section we briefly analyze the dynamics of a second-order PLL influenced by large-scale frequency variations with magnitude comparable to the PLL hold-in range.

We begin by considering a PLL based on a first-order low-pass loop filter followed by a nonlinear amplifier. We assume that the gain of the amplifier reduces with input voltage u as $K_{amp} = K_0/\sqrt{1 + (u/u_{sat})^2}$, where K_0 is the small-signal gain and u_{sat} is the saturation voltage. The product $K_0 u_{sat}$ corresponds to the maximum voltage at the amplifier output E_{max} , which is taken to be 10 V. We also assume that the PLL phase detector is based on an ideal mixer, so that its output voltage is a cosinusoidal function of the phase differ-

ence $\Delta\Phi$ between two oscillators: $u_{PD} = S_{PD} \cos(\Delta\Phi)$ where S_{PD} is the phase-to-voltage conversion ratio (for a typical microwave or RF mixer $S_{PD} \simeq 0.25$ V/rad).

Under the above assumptions, the characteristic equations of the PLL based on a first-order low-pass filter are given by¹⁸

$$\frac{du}{dt} + \frac{u}{\tau} = \frac{S_{PD}}{\tau} \cos(\Delta\Phi), \quad (3)$$

$$\frac{d\Delta\Phi}{dt} = \Delta\omega - \Omega_{max} \frac{u/u_{sat}}{\sqrt{1 + (u/u_{sat})^2}}, \quad (4)$$

where τ is the time constant of the low-pass filter, Ω_{max} is the PLL hold-in range, and $\Delta\omega$ characterizes the frequency difference between the master oscillator and a free-running slave. The parameters τ and Ω_{max} were taken to be 10 ms and 4 rad/s, respectively.

A solution of Eqs. (3) and (4) was sought assuming that $\Delta\omega$ is a random walk process. A typical time dependence of $\Delta\omega$, along with the corresponding solution for the “locked” phase difference $\Delta\Phi$, is shown in Fig. 9(a). The solution representing the amplifier output voltage $u_{amp} = K_{amp} \times u$ is shown in Fig. 9(b).

During the interval from 45 to 75 s, $\Delta\omega$ exceeds the PLL hold-in range, the PLL loses lock and misses 13 cycles (u_{amp} oscillates 13 times between $\pm E_{max}$), and then the PLL regains phase synchronism with the newly found stationary phase difference $\Delta\Phi = 53\pi/2$. Thus, this system is capable of restoring phase synchronism after losing it.

Most real life phase-locked loops contain integrators, and often two integrators in series are needed to cope with the laser frequency drifts caused by variations of ambient temperature. Next we consider the simplest case of a PLL based on an ideal integrator followed by a nonlinear amplifier. A system of characteristic equations of such a PLL is given by

$$\frac{du}{dt} + \frac{S_{PD}}{\tau} \sin(\Delta\Phi) \frac{d\Delta\Phi}{dt} = \frac{S_{PD}}{\tau} \cos(\Delta\Phi), \quad (5)$$

$$\frac{d\Delta\Phi}{dt} = \Delta\omega - \Omega_{max} \frac{u/u_{sat}}{\sqrt{1 + (u/u_{sat})^2}}, \quad (6)$$

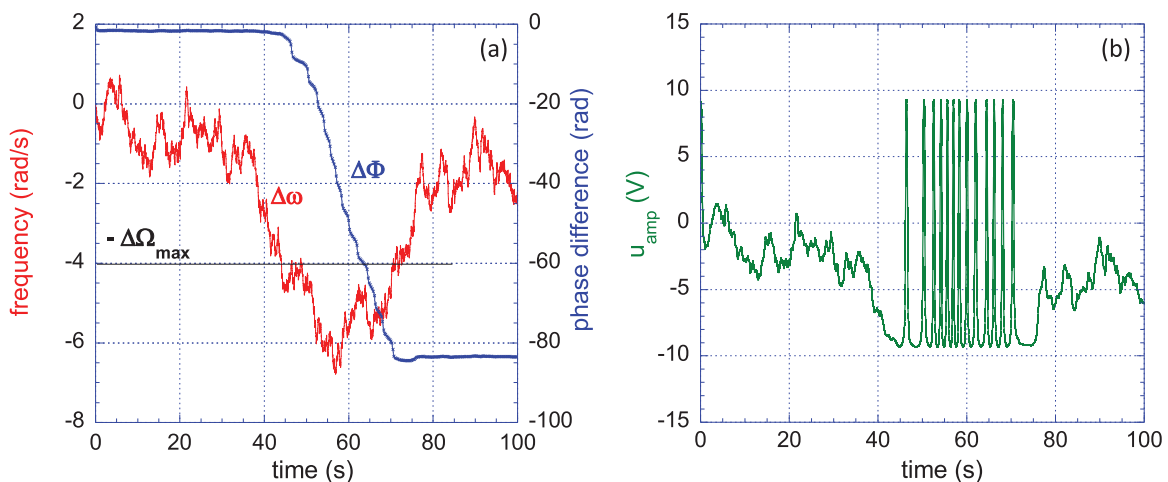


FIG. 9. (Color online) Dynamics of the PLL based on the first-order low-pass filter. (a) Frequency difference $\Delta\omega$ and phase difference $\Delta\Phi$. (b) PLL amplifier output voltage u_{amp} as a function of time.

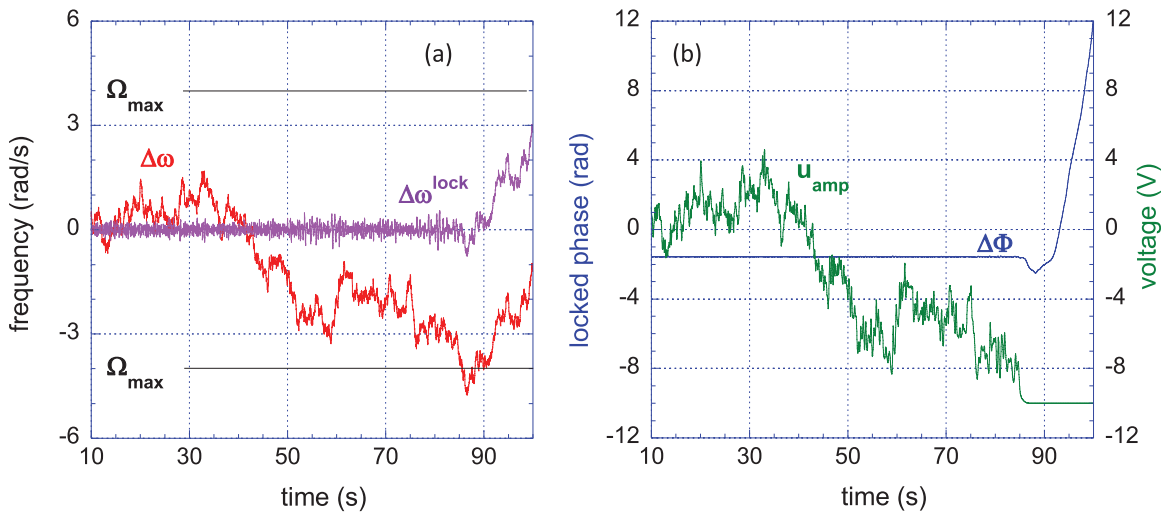


FIG. 10. (Color online) Dynamics of the PLL based on an ideal integrator. (a) Frequency difference between two oscillators $\Delta\omega$ (open- and close-loop control). (b) Closed-loop phase difference $\Delta\Phi$ and voltage at the output of the PLL amplifier u_{amp} as a function of time.

Once again, a solution of Eqs. (5) and (6) was sought assuming that $\Delta\omega$ is a random walk process, one possible realization of which is shown in Fig. 10(a). Also shown is the frequency difference between two phase-locked oscillators, $\Delta\omega^{lock}$. Here, the PLL maintains phase synchronism as long as $\Delta\omega$ does not exceed the hold-in range Ω_{max} . Slow variations of $\Delta\omega$ are suppressed and the noisy appearance of the trace $\Delta\omega^{lock}$ is due to spectral components of $\Delta\omega$ that are outside of the PLL bandwidth. $\Delta\Phi$ remains roughly constant ($\Delta\Phi = \int \Delta\omega^{lock} dt$), while the output voltage of the loop amplifier varies synchronously with $\Delta\omega$ (see Fig. 10(b)).

At $t = 85$ s, $\Delta\omega$ momentarily exceeds Ω_{max} and the PLL loses lock and does not recover, even when $\Delta\omega$ drops below Ω_{max} . This is due to the saturation of the loop nonlinear amplifier, which can be overcome only by resetting the PLL inte-

grator. The use of a frequency divider could prevent this loss of phase synchronism.

In addition to preventing the loss of phase-lock, a frequency divider can also reduce the burst-like noise induced by variations of $\Delta\omega$ with magnitude approaching the PLL hold-in range.¹⁴ We studied this noise mechanism by modeling sinusoidal variations of $\Delta\omega$. Figure 11 shows the “locked” phase difference between two oscillators computed at different values of the PLL bandwidth. As the PLL bandwidth progressively increases (traces 1, 2, and 3), the magnitude of the phase disturbances drops. Since it is not always possible to construct a PLL with sufficiently broad bandwidth to cope with these effects, limiting the magnitude of frequency variations via frequency division remains an attractive option.

V. CONCLUSION

We have studied the phase synchronization of diode lasers with high levels of frequency and phase fluctuations. The use of frequency dividers in phase-lock loops improves the reliability of the phase lock due to the reduced range of frequency variations without reducing the spectral purity of the lock. The use of frequency dividers does not eliminate the need for a broad bandwidth of the feedback control loop, if a high coherence between two offset phase-locked oscillators is required. Broadband phase noise suppression around the carrier is essential for avoiding an early carrier collapse when the signal frequency is multiplied.

ACKNOWLEDGMENTS

The authors thank J. Kitching for helpful discussions, S. Diddams for assistance with measurements, and J. M. Le Floch for supplying customized data acquisition software. This work is supported by the School of Physics of the University of Western Australia and the National Institute of Standards and Technology (NIST).

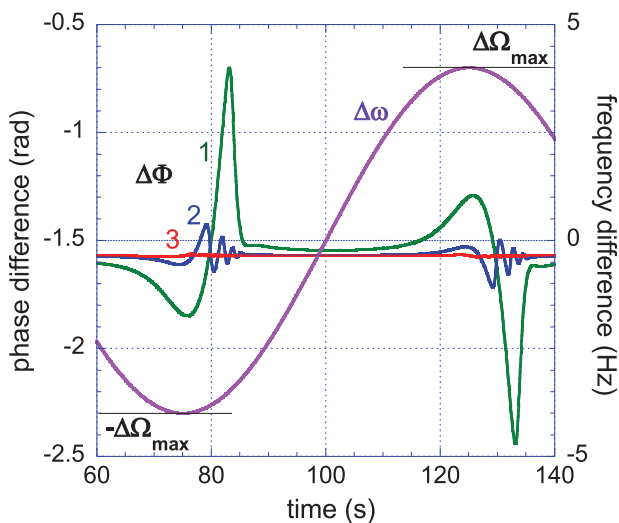


FIG. 11. (Color online) Effect of PLL bandwidth on the magnitude of phase disturbances caused by large-scale variations of $\Delta\omega$. Curves 1, 2, and 3 correspond to the “locked” phase difference computed for progressively increasing bandwidth of the phase control loop.

¹W. Liang, N. Satyan, F. Aflatouni, A. Yariv, A. Kewitsch, G. Rakuljic, and H. Hashemi, *J. Opt. Soc. Am. B* **24**, 2930 (2007).

- ²A. D. Cronin, J. Schmiedmayer, and D. E. Pritchard, *Rev. Mod. Phys.* **81**, 1051 (2009).
- ³M. M. Kash, V. A. Sautenkov, A. S. Zibrov, L. Hollberg, G. R. Welch, M. D. Lukin, Y. Rostovtsev, E. S. Fry, and M. O. Scully, *Phys. Rev. Lett.* **82**, 5229 (1999).
- ⁴I. Novikova, A. V. Gorshkov, D. F. Phillips, A. S. Sorensen, M. D. Lukin, and R. L. Walsworth, *Phys. Rev. Lett.* **98**, 243602 (2007).
- ⁵S. Knappe, V. Shah, P. D. D. Schwindt, L. Hollberg, and J. Kitching, *App. Phys. Lett.* **85**, 1460 (2004).
- ⁶P. Rabinowitz, J. Latourrette, and G. Gould, *Proc. IEEE* **51**, 857 (1963).
- ⁷J. Ye and J. L. Hall, *Opt. Lett.* **24**, 1838 (1999).
- ⁸A. M. Marino and J. C. R. Stroud, *Rev. Sci. Instrum.* **79**, 013104 (2008).
- ⁹Z. F. Fan, P. J. S. Heim, and M. Dagenais, *IEEE Photonics Technol. Lett.* **10**, 719 (1998).
- ¹⁰F. L. Walls and A. De Marchi, *IEEE Trans. Instrum. Meas.* **24**, 210 (1975).
- ¹¹E. Bava, A. De Marchi, and A. Godone, *IEEE Trans. Instrum. Meas.* **26**, 128 (1977).
- ¹²F.-X. Esnault, E. N. Ivanov, E. A. Donley, and J. Kitching, (unpublished).
- ¹³J. A. Barnes, A. R. Chi, L. S. Cutler, D. J. Healey, D. B. Leeson, T. E. McGunigal, J. A. Mullen, W. L. Smith, R. L. Sydnor, R. F. C. Vessot, and G. M. R. Winkler, *IEEE Trans. Instrum. Meas.* **IM-20**, 105 (1971).
- ¹⁴S. M. Foreman, A. D. Ludlow, M. H. G. de Miranda, J. E. Stalnaker, S. A. Diddams, and J. Ye, *Phys. Rev. Lett.* **99**, 153601 (2007).
- ¹⁵L. N. Langley, M. D. Elkin, C. Edge, M. J. Wale, U. Gliese, X. Huang, and A. J. Seeds, *IEEE Trans. Microwave Theory Tech.* **47**, 1257 (1999).
- ¹⁶M. Ohtsu, *Highly Coherent Semiconductor Lasers* (Artech House, Norwood, MA, 1992).
- ¹⁷F. J. Harris, *Proc. IEEE* **66**, 51 (1978).
- ¹⁸J. Kudrewicz and S. Wasowicz, *Equations of Phase-Locked Loops: Dynamics on the Circle, Torus and Cylinder* (World Scientific, Singapore, 2007).